Surgically Relevant Bony and Soft Tissue Anatomy of the Proximal Femur

Marc J. Philippon,*†‡ MD, Max P. Michalski,† MSc, Kevin J. Campbell,† BS, Mary T. Goldsmith,† MSc, Brian M. Devitt,† MD, Coen A. Wijdicks,† PhD, and Robert F. LaPrade,†‡ MD, PhD

Investigation performed at the Department of BioMedical Engineering of the Steadman Philippon Research Institute, Vail, Colorado, USA

Background: Hip endoscopy facilitates the treatment of extra-articular disorders of the proximal femur. Unfortunately, current knowledge of proximal femur anatomy is limited to qualitative descriptions and lacks surgically relevant landmarks.

Purpose: To provide a quantitative and qualitative analysis of proximal femur anatomy in reference to surgically relevant bony landmarks.

Study Design: Descriptive laboratory study.

Methods: Fourteen cadaveric hemipelvises were dissected. A coordinate measuring device measured dimensions and interrelationships of the gluteal muscles, hip external rotators, pectineus, iliopsoas, and joint capsule in reference to osseous landmarks.

Results: The vastus tubercle, superomedial border of the greater trochanter, and femoral head-neck junction were distinct and reliable osseous landmarks. The anteroinferior tip of the vastus tubercle was 17.1 mm (95% CI: 14.5, 19.8 mm) anteroinferior to the center of the gluteus medius lateral insertional footprint and was 22.9 mm (95% CI: 20.1, 25.7 mm) inferolateral to the center of the gluteus minimus insertional footprint. The insertions of the piriformis, conjoint tendon of the hip (superior gemellus, obturator internus, and inferior gemellus), and obturator externus were identified relative to the superomedial border of the greater trochanter. The relationship of the aforementioned footprints were 49% (95% CI: 43%, 54%), 42% (95% CI: 33%, 50%), and 64% (95% CI: 59%, 69%) from the anterior (0%) to posterior (100%) margins of the superomedial border of the greater trochanter, respectively. The hip joint capsule attached distally on the proximal femur 18.2 mm (95% CI: 14.2, 22.2 mm) from the head-neck junction medially on average.

Conclusion: The vastus tubercle, superomedial border of the greater trochanter, and the femoral head-neck junction were reliable osseous landmarks for the identification of the tendinous and hip capsular insertions on the proximal femur. Knowledge of the interrelationships between these structures is essential for endoscopic navigation and anatomic surgical repair and reconstruction.

Clinical Relevance: The qualitative and quantitative clinically relevant anatomic data presented here will aid in the diagnosis of proximal femur pathology and will provide a template for anatomic repair or reconstruction.

Keywords: hip endoscopy; external rotators; proximal femur; peritrochanteric surgical anatomy

Hip arthroscopy has experienced an exponential growth over the past 2 decades, as evidenced by advancement in diagnostic and surgical techniques.[5] The majority of procedures currently performed focus on the intra-articular structures, the acetabulum, and femoral head. However, as the field has evolved, the arthroscopic techniques developed are now being translated to facilitate the endoscopic treatment of extra-articular pathology of the proximal femur.

At present, endoscopic surgery in the peritrochanteric area involves the reattachment of gluteus medius and minimus tendons, bursal resections, iliotibial band releases, and treatment of piriformis and deep gluteal syndromes as a result of sciatic nerve entrapment by the piriformis, gemelli, and obturator internus muscles.[1,4,8,9,16,18,28,29] With the advancement in imaging and increase in peritrochanteric endoscopy, the external rotators of the hip (piriformis, gemelli, obturators, and quadratus femoris muscles) are being recognized as pain generators about the hip with successful long-term pain relief after release of the

*Address correspondence to Marc J. Philippon, MD, Steadman Philippon Research Institute, 181 West Meadow Drive, Suite 1000, Vail, CO 81657, USA (e-mail: mjp@sprivail.org).

† Steadman Philippon Research Institute, Vail, Colorado, USA.

‡ The Steadman Clinic, Vail, Colorado, USA.

One or more of the authors has declared the following potential conflict of interest or source of funding: R.F.L. is a consultant for Arthrex Inc. M.J.P. receives royalties from Smith & Nephew, Bledsoe, Donjoy, Arthrosurface, and ConMed Linvatex; is a paid consultant for Smith & Nephew and MIS; and has stock/stock options with Arthrosurface, Hipco, and MIS.

The Orthopaedic Journal of Sports Medicine, 2(6), 2325967114535188
DOI: 10.1177/2325967114535188

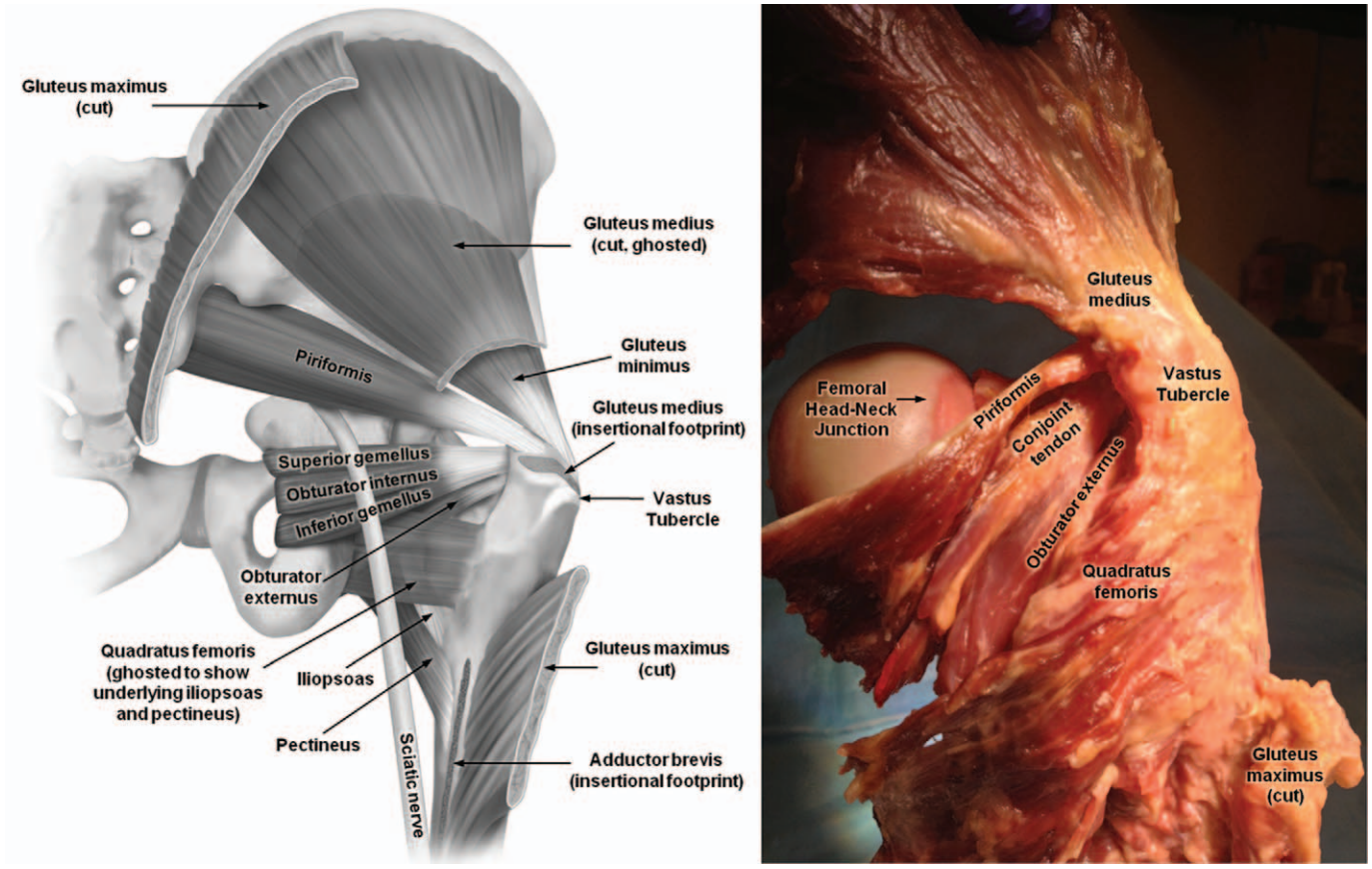

Figure 1. (Left) Illustration and (right) photograph of posterior view of right hemipelvis with muscles intact on the femur.

obturator internus in recalcitrant retrotrochanteric pain syndrome.[19,20,25,28] Additionally, endoscopy has an ever-increasing role in the diagnosis and treatment of recalcitrant postarthroplasty hip pain.[28] With this transition, the ever-expanding capabilities of hip arthroscopists and endoscopists are rapidly outpacing our knowledge of the precise locations of the clinically relevant anatomic structures of the proximal femur.

Today, only a small number of studies report anatomic information relevant to peritrochanteric endoscopy; however, most lack exact quantitative information regarding the spatial relationships of the proximal femur soft tissue attachments in reference to relevant endoscopic bony landmarks.[2,3,6,7,15,23] The purpose of this study was to advance the understanding of the clinically relevant proximal femur soft tissue attachment sites with a primary focus on endoscopically relevant osseous and soft tissue landmarks. This study aimed to provide a detailed qualitative and quantitative investigation of the areas, anatomic relationships, and insertions of muscles of the proximal femur and hip joint capsule with regard to pertinent bony landmarks. We hypothesized that consistent and reproducible distances and directions of the soft tissue attachments to the proximal femur could be elucidated in reference to clinically and endoscopically pertinent osseous landmarks.

MATERIALS AND METHODS

Pilot Study

Three fresh-frozen, nonpaired, proximal femurs were first dissected to verify the presence of reliable bony prominences and to define the optimal dissection approach. Prior to dissection, endoscopic evaluation was performed to confirm the ability to visualize and palpate the relevant osseous landmarks.

Specimen Preparation

Fourteen fresh-frozen, nonpaired, human cadaveric proximal femurs (mean age, 58 years; range, 47-65 years; mean body mass index, 24.6 kg/m^2; range, 19.2-32.1 kg/m^2; 12 male and 2 female, 8 right and 6 left) without evidence of prior injury, abnormality, or surgery were used for this study. Dissection commenced with removal of the skin, tensor fascia lata, and the sartorius muscle. All muscles attached to the proximal femur were isolated and excised through their midsubstance, which left the tendinous or muscular insertions intact. A qualitative assessment of the individual muscles was made in a systematic fashion from anterior to posterior. The short external rotator muscles, the superior gemellus, obturator internus, and inferior gemellus, had a common conjoint

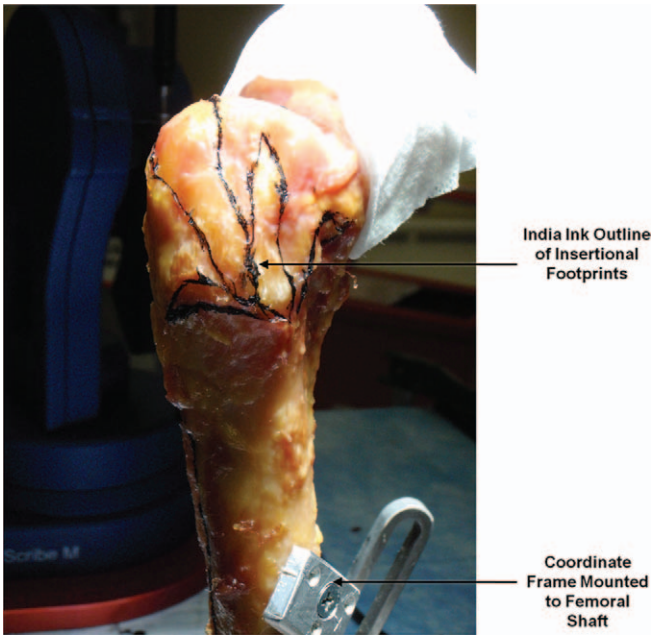

Figure 2. Photograph of a right hip demonstrating footprints of the muscular origins and insertions after fine dissection from the underlying osseous attachment while simultaneously outlining the locations using a fine-tipped calligraphy pen and India ink. This photograph demonstrates the India ink outlines of the gluteus medius and minimus insertions as well as the vastus lateralis insertion.

tendon. The additional tendinous structures not relevant to this study, including the adductor brevis, adductor longus, adductor magnus, vastus medialis, and vastus intermedius, were removed (Figure 1). A circumferential incision was made through the hip capsule at its midsubstance for disarticulation. The individual tendons of the proximal femoral musculature were carefully separated from each other and the capsule. Once isolated, each tendon was sharply dissected from its insertion while outlining the footprints with India ink using a fine-tipped calligraphy pen (Figure 2).

Data Collection

A coordinate measuring device (MicroScribe MX; GoMeasure3D, Amherst, Virginia, USA) with a previously reported[13] accuracy of 0.113 mm was used with a needle-point tip to collect anatomical locations. Data points were collected circumferentially along the inner border of the aforementioned India ink footprint outline. Data points were also taken along the superomedial border of the greater trochanter, the intertrochanteric crest, the head-neck junction of the femur, and along the vastus tubercle (Figures 3 and 4). The same individual performed the data collection for all specimens.

Coordinate System

A previously defined hip coordinate frame defined the directionality in the anatomic measurements of the proximal femur[24] that closely approximated the International Society for Biomechanics reporting standards.[30] Measurements encompassing the femoral head articular cartilage were obtained, and a best-fit sphere was used to determine the femoral head center. Data points taken about the long axis of the femoral shaft defined the superior/inferior axis. A line perpendicular to the femoral axis and which intersected the center of the femoral head was used to define the medial/lateral axis. The anterior/posterior direction was defined by the axis mutually perpendicular to the other axes. A clock-face coordinate system was generated from a best-fit circle of the head-neck junction data defined by the superior-most point as 12 o'clock and with 3 o'clock directed anteriorly for a right hip.

Data Analysis

Data were analyzed using custom software (MATLAB 2008b; MathWorks Inc, Natick, Massachusetts, USA). The muscular insertion footprint areas were calculated using the Heron formula[21]; the average footprint center was used as the primary reference point for each insertion. Area and distance measurements are reported as averages with 95% CIs, which were calculated using the appropriate t score. For distance measurements, the primary direction was reported for each 3-dimensional distance.

RESULTS

Individual soft tissue and osseous structures of the proximal femur are described. For each subsection, a qualitative description of the specific structure is provided followed by quantitative measurements. The measurements are the mean values with 95% CIs for all the anatomic structures unless stated otherwise. The footprint areas and morphology of each muscular insertion are described in Table 1. The interrelationships of the soft tissues and osseous landmarks are detailed in Table 2.

Osseous Landmarks

Vastus Tubercle. The vastus tubercle formed an arching prominence located on the lateral aspect of the femur, immediately deep to the origin of the vastus lateralis (Figures 1 and 5). The vastus tubercle was clearly identifiable underlying the shiny appearing longitudinal fibers of the vastus lateralis, which occupied the entire length of the arch from anterior to posterior. The anteroinferior apex of the ridge formed a distinctly palpable and endoscopically visible tubercle that marked the most anteroinferior insertion of the gluteus medius muscle, which blended with the nearby lateral apex of the gluteus minimus.

Superomedial Border of the Greater Trochanter. The anterior and posterior tips of the greater trochanter were connected by a bony crest, which was referred to as the superomedial border of the greater trochanter (Figures 3 and 4). This crest demarcated the division of the gluteus medius and gluteus minimus tendon insertions laterally from the external rotator (piriformis, conjoint tendon of

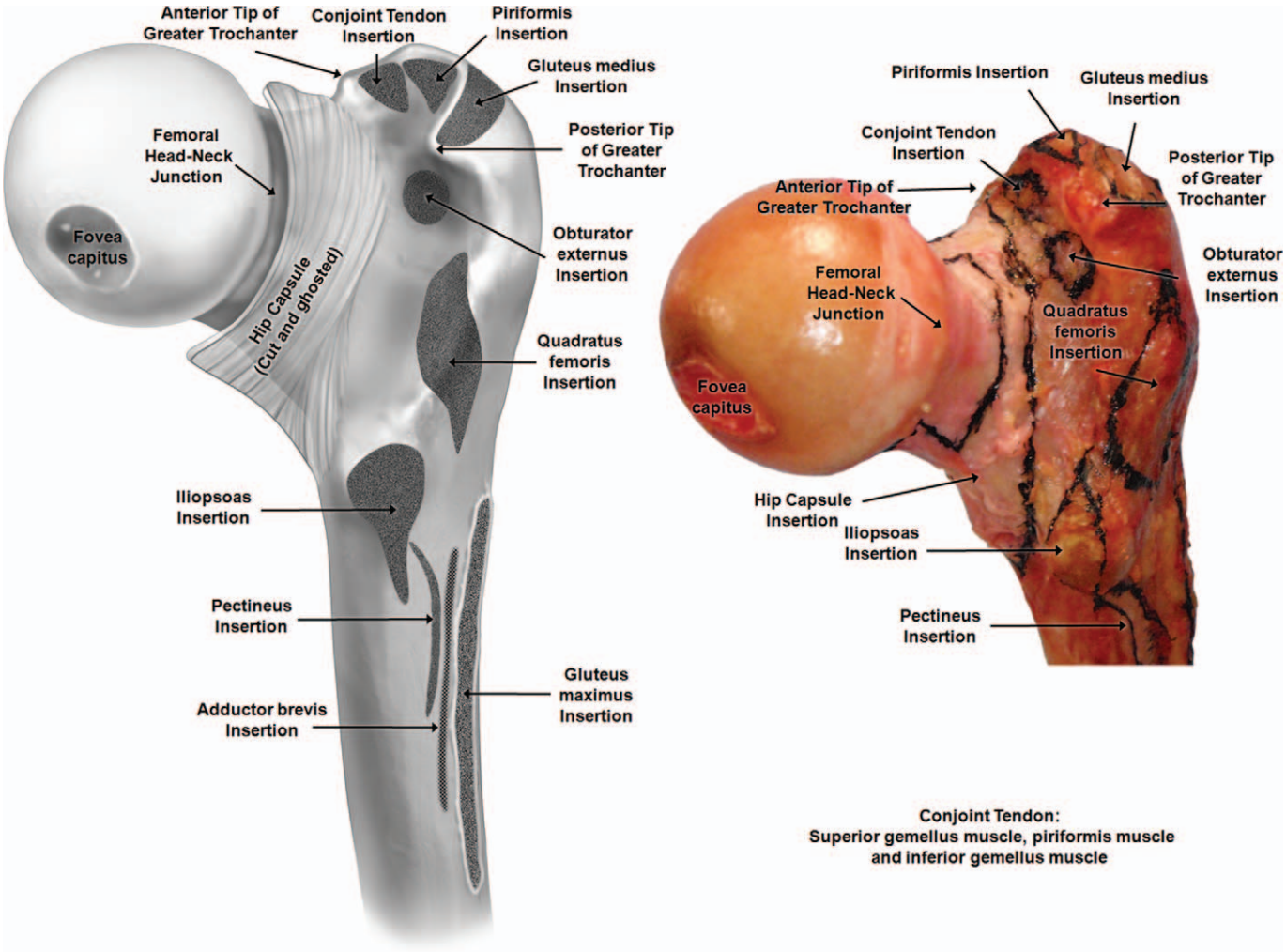

Figure 3. (Left) Illustration and (right) photograph of the posteromedial proximal femur of a left hip looking anterolaterally at the footprint insertions on the medial surface of the greater trochanter and posterior proximal femur.

superior gemellus, obturator internus, inferior gemellus, and obturator externus) insertions medially.

Femoral Head-Neck Junction. The head-neck junction of the femur was identified as the confluence between the convex articular cartilage surface of the femoral head and the slightly concave surface of the femoral neck (Figure 4).

Soft Tissue Attachments

Gluteus Maximus. The gluteus maximus had a broad, robust attachment onto the femur at the site of the linea aspera. The adductor brevis tendon was located medial to the gluteus maximus insertion, separating it from the tendon of the pectineus muscle.

The length of the gluteus maximus muscular insertion on the linea aspera was 74.9 mm (95% CI: 67.1, 82.8). The superior apex of the footprint was located 19.2 mm (95% CI: 15.1, 23.3) posterior, inferior, and medial to the posteroinferior vastus tubercle.

Gluteus Medius. The gluteus medius insertional footprint was located on the lateral aspect of the greater trochanter. It comprised the lateral and superomedial insertions. At the anteroinferior corner of the lateral facet, the gluteus medius footprint was adjacent to the lateral border of the gluteus minimus and had interdigitating fibers, which created a small area of overlap between the 2 tendon insertions (Figure 5). The superomedial facet extended posteriorly to the posterior tip of the greater trochanter. The anterior and posterior borders of the lateral and superomedial facets were contiguous and measured 58.6 mm (95% CI: 52.4, 64.7 mm) and 63.2 mm (95% CI: 58.9, 67.6 mm) in length, respectively.

Gluteus Minimus. The gluteus minimus muscle attached onto the anterior aspect of the greater trochanter with a long, thin tendinous insertion. Two distinct footprint attachment morphologies were observed during dissection: a single crescent (11/14) or a bowtie configuration (3/14). The lateral facet of the bowtie footprint was located inferior to the vastus tubercle. The most superomedial aspect of the gluteus minimus tendon was intimately associated with the joint capsule and interdigitated with the fibers of the conjoint and piriformis tendons. The inferior border of the gluteus minimus

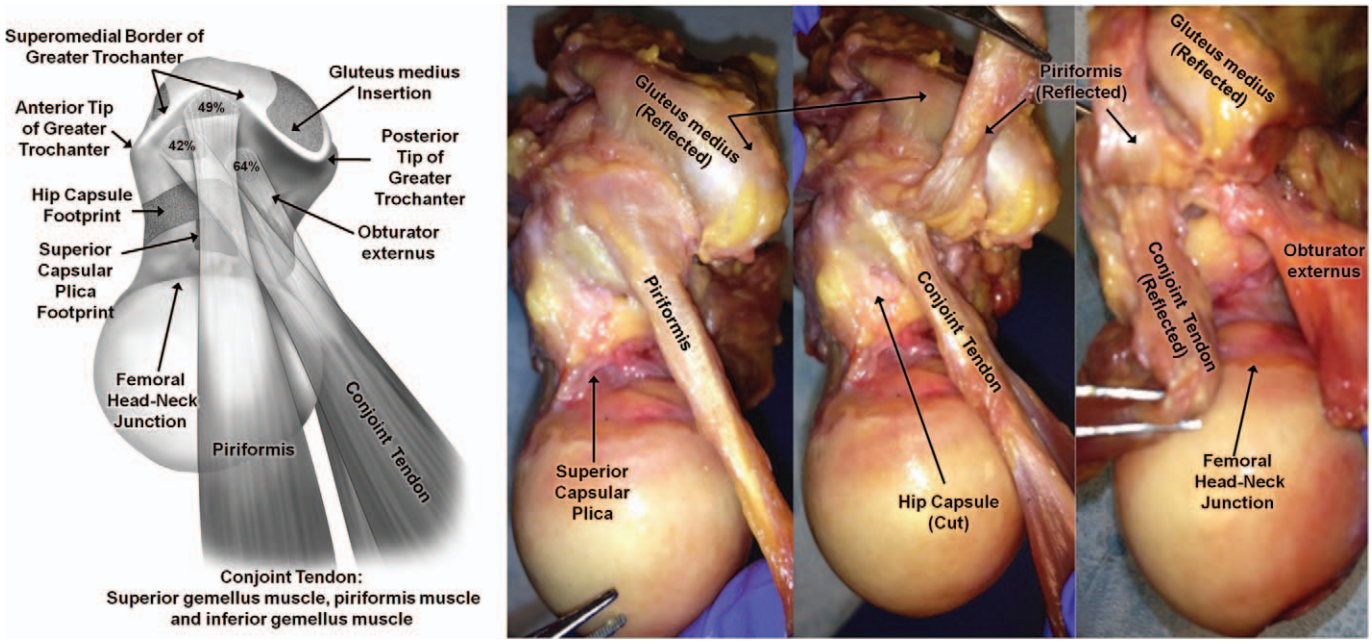

Figure 4. (Left) Illustration and (right) photograph of superior view looking inferiorly at the femoral head, femoral neck, and greater trochanter of a right hip. The insertions of the piriformis, conjoint tendon (superior gemellus, obturator internus, and inferior gemellus), and obturator externus with respect to the superomedial border of the greater trochanter are depicted.

TABLE 1
Footprint Area and Morphology of Proximal Femur Musculature

	Average Area, mm^2 (95% CI)	Description of Insertion
Gluteus maximus	473.4 (381.0, 565.8)	Thick, muscular insertion along the posterior femur on the linea aspera
Gluteus medius		
Lateral facet	141.1 (117.7, 164.5)	Composed of 2 contiguous rectangular footprints, the lateral facet oriented in the sagittal plane and
Superomedial facet	501.5 (442.8, 560.2)	the superomedial facet primarily in the transverse plane
Gluteus minimus	280.9 (229.3, 332.5)	Two morphologies noted: The majority (11/14) were long, thin, and crescent shaped and ran medial to lateral and concave facing inferiorly, while a few (3/14) were bowtie in shape
Piriformis	58.7 (50.5, 66.9)	Triangular, tendinous insertion with anterior, posterior, and lateral apices
Conjoint tendon	53.6 (37.1, 70.2)	Triangular, tendinous insertion with anterior, posterior, and lateral apices
Obturator externus	56.1 (46.0, 66.2)	Circular muscular insertion
Quadratus femoris	366.4 (297.3, 435.6)	Muscular, teardrop-shaped insertion
Iliopsoas	359.5 (305.9, 413.0)	Inverted teardrop shape, circular tendinous psoas and thin muscular iliacus insertions
Pectineus	232.9 (157.6, 308.2)	Thin, musculotendinous, crescent-shaped insertion facing concave inferomedially

inserted onto a bony ridge that separated it from the most superior fibers of the vastus intermedius origin.

The center of the footprint was 19.6 mm (95% CI: 16.7, 22.5 mm) inferolateral to the anterior tip of the greater trochanter and 22.9 mm (95% CI: 20.1, 25.7 mm) superomedial to the anteroinferior vastus tubercle. The lateralmost point of the gluteus minimus footprint was 11.6 mm (95% CI: 8.0, 15.2 mm) from the anteroinferior corner of the gluteus medius.

Piriformis Tendon. The piriformis inserted onto a small fossa located immediately medial and inferior to the superomedial border of the greater trochanter. The piriformis footprint was centered in the anteroposterior axis of the greater trochanter (Table 2). The tendon was closely associated with the conjoint tendon, with fibroconnective tissue interdigitations present in all cases.

The center and most lateral point of the piriformis footprint were 49% (95% CI: 43%, 54%) and 48% (95% CI: 42%,

TABLE 2
Interrelationships of Soft Tissues With Respect to Osseous Landmarks[a]

	Total	Anterior (–)/ Posterior (+)	Superior (+)/ Inferior (–)	Medial (–)/ Lateral (+)
Gluteus maximus				
Superior apex to posteroinferior VT	19.2 (15.1, 23.3)	(–)7.0 (4.3, 9.8)	16.2 (12.5, 19.9)	5.7 (3.6, 7.8)
Superior apex to inferior apex	74.9 (67.1, 82.8)	1.4 (–1.4, 4.1)	(–)74.4 (66.5, 82.3)	(–)6.5 (4.3, 8.6)
Gluteus medius				
Superomedial footprint center to posterior tip of GT	17.0 (15.4, 18.6)	10.4 (9.2, 11.7)	5.1 (3.8, 6.3)	(–)12.1 (10.6, 13.5)
Posterosuperior corner to posterior tip of GT	4.2 (3.0, 5.3)	1.8 (0.1, 3.5)	0.3 (–0.8, 1.4)	(–)1.2 (–0.2, 2.6)
Lateral footprint center to anteroinferior VT	17.1 (14.5, 19.8)	(–)2.4 (–0.8, 5.6)	(–)15.3 (12.9, 17.7)	(–)3.1 (0.5, 5.7)
Anterior inferior corner to anteroinferior VT	11.1 (7.8, 14.4)	(–)0.7 (–2.9, 4.2)	(–)8.5 (5.7, 11.3)	(–)3.0 (0.8, 5.2)
Gluteus minimus				
Center to anterior tip of GT	19.6 (16.7, 22.5)	(–)0.3 (–2.4, 3.1)	13.1 (8.2, 18.0)	(–)10.9 (7.6, 14.2)
Superomedial apex to anterior tip of GT	9.4 (6.0, 12.8)	(–)1.8 (–0.8, 4.4)	(–)3.8 (0.3, 7.3)	(–)4.3 (1.0, 7.7)
Center to anteroinferior VT	22.9 (20.1, 25.7)	4.2 (2.2, 6.2)	(–)20.0 (16.5, 23.6)	7.8 (5.1, 10.5)
Inferolateral apex to anteroinferior VT	10.2 (7.0, 13.4)	2.9 (1.2, 4.5)	(–)3.7 (–0.3, 7.7)	5.1 (1.7, 8.6)
Inferolateral apex to anteroinferior corner of GM	11.6 (8.0, 15.2)	3.6 (0.8, 6.3)	4.8 (2.1, 7.6)	8.2 (5.1, 11.2)
Piriformis				
Anterior apex to posterior apex	13.8 (12.2, 15.4)			
Center to anterior tip of GT	19.4 (15.3, 23.5)	(–)14.8 (11.9, 17.7)	(–)9.6 (6.0, 13.2)	(–)4.4 (1.1, 7.7)
Center to posterior tip of GT	20.2 (17.5, 22.8)	18.9 (16.5, 21.3)	(–)0.4 (–2.1, 2.9)	(–)4.3 (1.9, 6.7)
Conjoint tendon of hip				
Center to anterior tip of GT	16.8 (12.2, 21.4)	(–)13.1 (9.5, 16.7)	(–)4.7 (0.2, 9.1)	0.0 (–4.5, 4.5)
Center to center of piriformis	10.4 (9.2, 11.6)	1.7 (–2.1, 5.5)	4.9 (2.7, 7.2)	4.4 (2.5, 6.3)
Obturator externus				
Center to anterior tip of GT	27.7 (25.6, 29.9)	(–)24.5 (21.8, 27.1)	7.5 (3.1, 11.8)	(–)0.9 (–3.5, 5.3)
Center to posterior tip of GT	19.5 (18.1, 21.0)	9.3 (7.8, 10.8)	16.7 (14.9, 18.5)	(–)0.7 (–0.9, 2.3)
Center to center of conjoint tendon	17.5 (15.4, 19.6)	(–)11.3 (8.5, 14.2)	12.1 (10.1, 14.1)	(–)0.8 (–1.0, 2.7)
Quadratus femoris				
Superior apex to inferior apex	40.0 (34.9, 45.1)	2.3 (–0.3, 4.9)	(–)39.0 (33.7, 44.4)	(–)3.4 (–0.1, 6.8)
Inferior apex to superior tip of linea aspera	20.1 (16.1, 24.2)	(–)8.3 (5.8, 10.7)	(–)1.4 (–4.2, 7.0)	14.2 (9.0, 19.4)
Superior capsular plicae				
Anteromedial apex to posteromedial apex	13.9 (11.7, 16.2)			
Anterolateral apex to posterolateral apex	13.3 (10.7, 15.8)			
Inferior capsular plicae				
Anteromedial apex to posteromedial apex	9.8 (7.4, 12.1)			
Anterolateral apex to posterolateral apex	9.2 (7.2, 11.3)			

[a]Values are in millimeters and are expressed as average (95% CI). GM, gluteus medius; GT, greater trochanter; VT, vastus tubercle.

55%) of the distance from the anterior tip (0%) to posterior tip (100%) of the greater trochanter, respectively.

Proximal Femur Conjoint Tendon (Superior Gemellus, Obturator Internus, Inferior Gemellus). The conjoint tendon of the hip was formed as a coalescence of the superior gemellus, obturator internus, and inferior gemellus muscles. The tendons of the superior gemellus, obturator internus, and inferior gemellus originated medially but formed a single uniform tendon laterally at the posterior head-neck junction of the femur. The tendon inserted on the medial surface of the greater trochanter. The individual muscles were distinguishable by separate muscle bellies posteriorly but could not be divided at their tendinous insertion (Figure 4). This conjoint tendon passed obliquely inferior and anterior to the piriformis tendon to its insertion near the anterior tip of the greater trochanter. The center of the conjoint tendon footprint was 42% (95% CI: 33%, 50%) of the distance from the anterior tip (0%) to posterior tip (100%) of the greater trochanter.

Obturator Externus. The obturator externus muscle had an oval-shaped footprint, forming a small recess located at the junction of the posterior femoral neck and the medial face of the greater trochanter in the obturator fossa. The muscular belly of the obturator externus ran immediately deep (anterior) to the quadratus femoris and coursed superiorly to its insertion. There was a thick, tendinous insertion, which created a groove in the posterior aspect of the femoral neck. The center of the obturator externus tendon footprint was 64% (95% CI: 59%, 69%) of the distance from the anterior tip (0%) to posterior tip (100%) of the greater trochanter.

Quadratus Femoris. The quadratus femoris had a broad teardrop-shaped muscular insertion on the posterior femur partially overlying the inferior margin intertrochanteric crest. The muscle belly was rectangular in shape and covered the posterior margin of the obturator externus. It separated the lesser trochanter from the structures on the posterior aspect of the proximal femur.

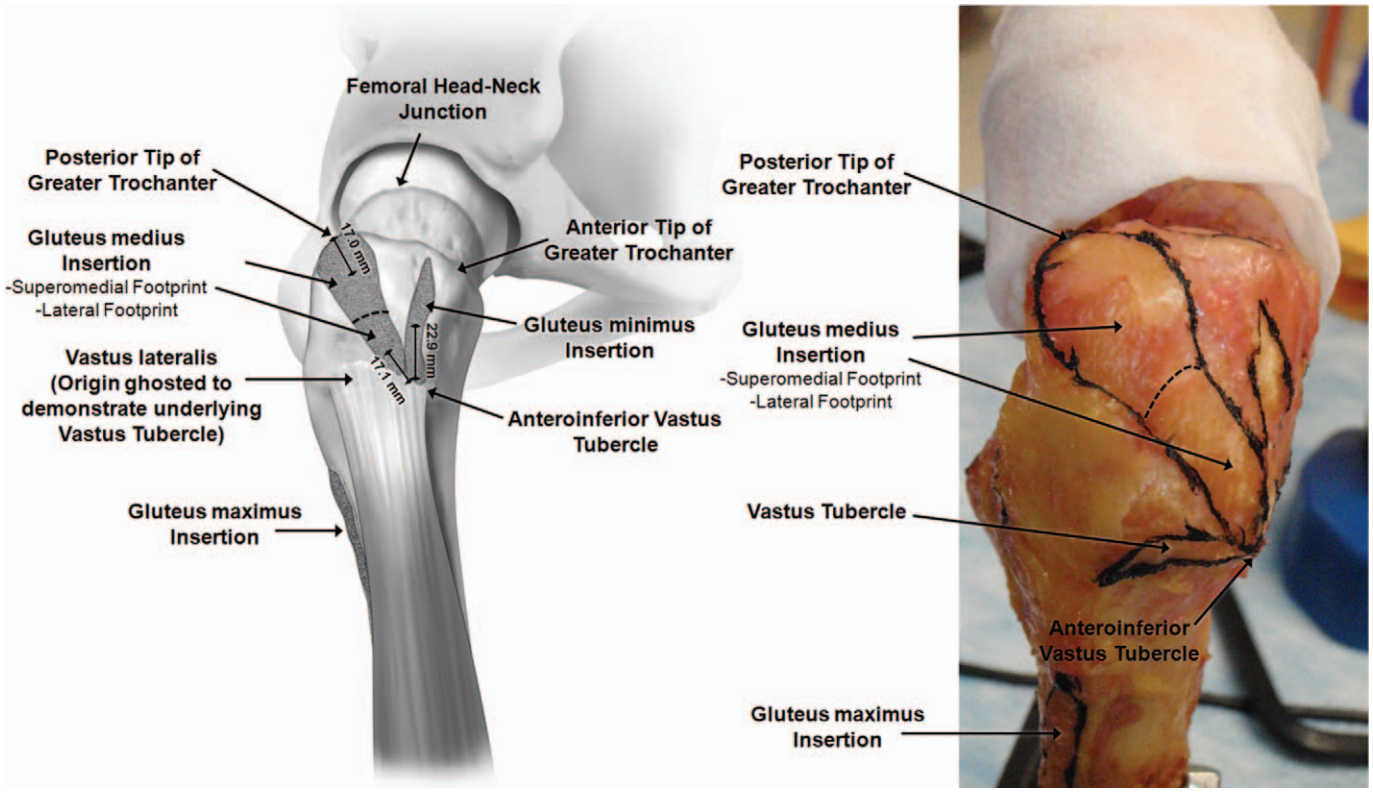

Figure 5. (Left) Illustration and (right) photograph of lateral view of a right hip looking medially at the footprint insertions of the greater trochanter. The footprints of the gluteus medius, gluteus minimus, and vastus lateralis with respect to the vastus tubercle are depicted.

TABLE 3
Capsular Width and Distance to Head-Neck Junction of the Femur With Respect to Clock-Face Position[a]

Clock-Face Position[b]	Distance From Head-Neck Junction to Capsule, mm	Width of Capsule, mm
12:00	9.3 (5.9, 12.7)	11.8 (9.2, 14.4)
1:00	17.6 (12.4, 22.9)	12.1 (10.1, 14.1)
2:00	21.9 (17.8, 25.9)	10.1 (8.6, 11.7)
3:00	22.4 (18.6, 26.2)	10.8 (9.2, 12.3)
4:00	21.9 (18.3, 25.5)	12.9 (10.3, 15.5)
5:00	22.6 (19.4, 25.8)	14.4 (12.2, 16.6)
6:00	22.9 (20.2, 25.6)	18.9 (14.5, 23.2)
7:00	18.8 (15.6, 22.1)	12.2 (7.9, 16.6)
8:00	17.0 (14.3, 19.7)	5.6 (3.9, 7.3)
9:00	16.1 (12.8, 19.4)	4.8 (3.3, 6.4)
10:00	15.2 (11.8, 18.6)	5.5 (3.7, 7.3)
11:00	11.0 (7.3, 14.8)	10.2 (7.9, 12.5)

[a]Values are expressed as average (95% CI).
[b]12:00 = superior; 3:00 = anterior; 6:00 = inferior; 9:00 = posterior.

The superoinferior length of the muscular insertion was 40.0 mm (95% CI: 34.9, 45.1 mm). The inferior margin of the footprint was 20.1 mm (95% CI: 16.1, 24.2 mm) posteromedial to the superior tip of the linea aspera.

Iliopsoas. The iliopsoas had an inverted teardrop-shaped insertion occupying the entire posterior surface of the lesser trochanter, extending to the junction of the inferior lesser trochanter with the femoral shaft. The superior margin of the iliopsoas insertion was closely related to the inferiormost insertion of the joint capsule.

Pectineus. The pectineus insertion was crescent-shaped with its concave border facing inferomedially and convex border face superolaterally. The pectineus had a very long and thin tendinous sheath-like insertion, which approached the inferior concave posterior edge of the lesser trochanter (Figure 3). Coursing inferiorly, the footprint veered laterally toward the insertion of the adductor brevis and the insertion of the gluteus maximus on the linea aspera.

Joint Capsule and Capsular Plicae. The joint capsule inserted circumferentially around the femoral neck, along the intertrochanteric line anteriorly and intertrochanteric crest posteriorly. The thickness and distance from the head-neck junction of the capsule was variable according to the clock-face position of the head-neck junction and are provided in Table 3.

In addition to the joint capsule, superior and inferior plicae (ligaments of Weibrecht) were noted in 13/14 (93%) and 10/14 (71%) specimens, respectively. Utilizing the clock-face coordinate system generated about the head-neck junction, the superior plicae spanned from clock-face position

10:30 to 12:30, and the inferior plicae spanned from clockface position 6:30 to 7:30.

DISCUSSION

The most important clinically relevant findings of this study were the interrelationships of 3 distinct osseous structures (the vastus tubercle, the superomedial ridge of the greater trochanter, and the femoral head-neck junction) with respect to the surrounding soft tissues, which can provide an anatomically based surgical guide for the location of pertinent extra-articular soft tissue structures endoscopically. Advances in imaging modalities and a heightened clinical suspicion have increased awareness and recognition of peritrochanteric pathology as a cause of hip pain and functional impairment.[8,9,14,16-20,25,27,29] The data provided in this study not only enhance the current understanding of anatomy of the peritrochanteric space and proximal femur but also provide endoscopically relevant landmarks to aid in navigation and provide a surgical map for anatomical reconstruction.

A key deliberation in the methodology of this study was to provide clinically meaningful measurements in relation to clearly identifiable structures. Therefore, in choosing specific bony landmarks, it was imperative that they were either clearly visible or palpable during endoscopy. This is in contrast to previous anatomical studies that have focused on open surgical or arthroplasty techniques.[10-12,22,26] The vastus tubercle has recently been qualitatively reported as a reference point for evaluation of peritrochanteric pathology.[29] The presence of the shiny white fibers of the vastus lateralis in direct continuity with this bony prominence provides a distinct and reliable reference point.[29] Given that the space in this area is restricted because of lateral restraint of the tensor fascia lata, it is often challenging to visualize the muscle belly of the gluteus medius in continuity. The identification of the posterior and anterior tips of the superomedial greater trochanter, and the interposed superomedial ridge, are valuable landmarks to define the borders and center of the superomedial facet, which is an especially important landmark for arthroscopic repairs of the gluteus medius tendon. Furthermore, the quantitative data provided for the footprint of the gluteus medius may simplify the decision on how best to re-create this attachment with anchor placement to reproduce the native anatomy when it is repaired. This is particularly applicable when performing a suture bridge or similar technique to repair abductor muscle tears, which reportedly require placement of medial and lateral rows of suture anchors.[8,9] While there is no current consensus regarding the optimal treatment of partial tears of the gluteus medius, which are now being reported with a prevalence of up to 10% and 25% of middle-aged men and women, respectively,[8] a quantitative understanding of the tendinous insertion may influence clinical decision making regarding operative versus nonoperative management.

In analyzing the structures of the proximal femur, current diagnosis of pathology in this area and the indications for treatment are limited, at best, and frequently the subject of conjecture. Encouragingly, the anatomic information provided in this study can be used as an anatomic template for normal anatomy and aid in deciphering the cause of undifferentiated groin pain and abnormalities in hip motion. It should also be considered that, whereas this study was focused primarily on determining the endoscopically relevant anatomy, the findings are not exclusive to this surgical technique, and the revelations, particularly as they relate to the location of the conjoint tendon and piriformis, may be even more relevant to the fields of trauma and hip arthroplasty to prevent iatrogenic injury.

The results of our study concur with previous studies that describe the anatomy of the gluteus medius, gluteus minimus, and short external rotators of the hip. Robertson et al[24] described insertional footprints of the gluteus medius and minimus. They reported the footprint areas of the superomedial (438 mm^2) and lateral (196 mm^2) footprints. Our findings corroborate the measurement of the lateral footprint but differed regarding the superomedial footprint because Robertson et al[24] used a best-fit circle, whereas we utilized the Heron formula[21] and found a larger area for the roughly rectangular-shaped footprint. Additionally, there was a similarity in the qualitative observations of the gluteus minimus insertion, which they described in their report as consisting of a capsular head and a long head and a pattern we likened to a "bowtie footprint," albeit this finding was only recognized in a minority of our specimens (3/14). Ito et al[11] and Pine et al[22] have reported qualitative descriptions of the short external rotators from the perspective of an open approach after dislocation and following an osteotomy of the femoral neck. Our study as well as these studies employed the concept of an anteroposterior span of the medial face of the greater trochanter to describe the relative insertions of the piriformis and conjoint tendon. We reported that the conjoint tendon of the superior gemellus, obturator internus, and inferior gemellus inserted anterior to the insertion of the piriformis, which is in agreement.[11,22]

There were some limitations to this study. The number of specimens was limited, and prescreening of specimens with radiological imaging was not performed. The current study's specimen quantity was similar to the numbers used in previously published anatomic studies. Although no imaging was performed, grossly abnormal specimens were not identified during dissections. In addition, hemipelvises were used in this study because it allowed isolation of entire muscle origins to follow the muscle belly and tendons to accurately identify their insertions. The fresh-frozen cadavers had a maximum age of 65 years, thereby theoretically minimizing the inclusion of the specimens with tissue atrophy and bony abnormalities.

CONCLUSION

The vastus tubercle, the superomedial border of the greater trochanter, and the femoral head-neck junction provided valuable and reliable osseous landmarks for the identification of the tendinous and capsular insertions on the proximal femur. Knowledge of the interrelationship between

these structures is essential for endoscopic navigation and anatomic surgical repair, and reconstruction of the musculature of the proximal femur and the information presented in this report will serve as an anatomic guide for these procedures. While aimed at endoscopically relevant landmarks, a quantitative description of the anatomy of the proximal femur can be implemented in numerous subspecialties in orthopaedic surgery, including but not limited to sports medicine, joint replacement, and trauma.

REFERENCES

1. Barnthouse NC, Wente TM, Voos JE. Greater trochanteric pain syndrome: endoscopic treatment options. *Oper Tech Sports Med*. 2012;20:320-324.
2. Beck M, Sledge JB, Gautier E, Dora CF, Ganz R. The anatomy and function of the gluteus minimus muscle. *J Bone Joint Surg Br*. 2000; 82:358-363.
3. Bedi A, Galano G, Walsh C, Kelly BT. Capsular management during hip arthroscopy: from femoroacetabular impingement to instability. *Arthroscopy*. 2011;27:1720-1731.
4. Berthelot J-M, Potaux F, Alliaume C, Prost A, Maugars Y. A case of hip rotator cuff tear revealed by refractory gluteus medius tendinosis. *Joint Bone Spine*. 2001;68:360-363.
5. Colvin AC, Harrast J, Harner C. Trends in hip arthroscopy. *J Bone Joint Surg Am*. 2012;94:e23.
6. Dienst M. Hip arthroscopy: technique and anatomy. *Oper Tech Sports Med*. 2005;13:13-23.
7. Dienst M, Godde S, Seil R, Hammer D, Kohn D. Hip arthroscopy without traction: in vivo anatomy of the peripheral hip joint cavity. *Arthroscopy*. 2001;17:924-931.
8. Domb BG, Botser I, Giordano BD. Outcomes of endoscopic gluteus medius repair with minimum 2-year follow-up. *Am J Sports Med*. 2013;41:988-997.
9. Domb BG, Nasser RM, Botser IB. Partial-thickness tears of the gluteus medius: rationale and technique for trans-tendinous endoscopic repair. *Arthroscopy*. 2010;26:1697-1705.
10. Flack NA, Nicholson HD, Woodley SJ. The anatomy of the hip abductor muscles. *Clin Anat*. 2014;27:241-253.
11. Ito Y, Matsushita I, Watanabe H, Kimura T. Anatomic mapping of short external rotators shows the limit of their preservation during total hip arthroplasty. *Clin Orthop Relat Res*. 2012;470:1690-1695.
12. Iyem C, Guvencer M, Karatosun V, Unver B. Morphometric evaluation of proximal femur in patients with unilateral total hip prosthesis. *Clin Anat*. 2014;27:478-488.
13. Johannsen AM, Civitarese DM, Padalecki JR, Goldsmith MT, Wijdicks CA, LaPrade RF. Qualitative and quantitative anatomic analysis of the posterior root attachments of the medial and lateral menisci. *Am J Sports Med*. 2012;40:2342-2347.
14. Kagan A 2nd. Rotator cuff tears of the hip. *Clin Orthop Relat Res*. 1999;(368):135-140.
15. Keene GS, Villar RN. Arthroscopic anatomy of the hip: an in vivo study. *Arthroscopy*. 1994;10:392-399.
16. Lachiewicz PF. Abductor tendon tears of the hip: evaluation and management. *J Am Acad Orthop Surg*. 2011;19:385-391.
17. Lequesne M, Djian P, Vuillemin V, Mathieu P. Prospective study of refractory greater trochanter pain syndrome. MRI findings of gluteal tendon tears seen at surgery. Clinical and MRI results of tendon repair. *Joint Bone Spine*. 2008;75:458-464.
18. Martin HD, Shears SA, Johnson JC, Smathers AM, Palmer IJ. The endoscopic treatment of sciatic nerve entrapment/deep gluteal syndrome. *Arthroscopy*. 2011;27:172-181.
19. Meknas K, Christensen A, Johansen O. The internal obturator muscle may cause sciatic pain. *Pain*. 2003;104:375-380.
20. Meknas K, Kartus J, Letto JI, Christensen A, Johansen O. Surgical release of the internal obturator tendon for the treatment of retrotrochanteric pain syndrome: a prospective randomized study, with long-term follow-up. *Knee Surg Sports Traumatol Arthrosc*. 2009; 17:1249-1256.
21. Nelsen RB. Heron's formula via proofs without words. *Coll Mathematics J*. 2001;32:290-292.
22. Pine J, Binns M, Wright P, Soames R. Piriformis and obturator internus morphology: a cadaveric study. *Clin Anat*. 2011;24:70-76.
23. Ranawat AS, Kelly BT. Anatomy of the hip: open and arthroscopic structure and function. *Oper Tech Orthop*. 2005;15:160-174.
24. Robertson WJ, Gardner MJ, Barker JU, Boraiah S, Lorich DG, Kelly BT. Anatomy and dimensions of the gluteus medius tendon insertion. *Arthroscopy*. 2008;24:130-136.
25. Robinson G, Hine AL, Richards PJ, Heron CW. MRI abnormalities of the external rotator muscles of the hip. *Clin Radiol*. 2005;60: 401-406.
26. Solomon LB, Lee YC, Callary SA, Beck M, Howie DW. Anatomy of piriformis, obturator internus and obturator externus: implications for the posterior surgical approach to the hip. *J Bone Joint Surg Br*. 2010;92: 1317-1324.
27. Stafford GH, Villar RN. Ischiofemoral impingement. *J Bone Joint Surg Br*. 2011;93:1300-1302.
28. Verhelst L, Guevara V, De Schepper J, Van Melkebeek J, Pattyn C, Audenaert EA. Extra-articular hip endoscopy: a review of the literature. *Bone Joint Res*. 2012;1:324-332.
29. Voos JE, Rudzki JR, Shindle MK, Martin H, Kelly BT. Arthroscopic anatomy and surgical techniques for peritrochanteric space disorders in the hip. *Arthroscopy*. 2007;23:1246.e1241-e1245.
30. Wu G, Siegler S, Allard P, et al. Standardization, Terminology Committee of the International Society of Biomechanics. ISB recommendation on definitions of joint coordinate system of various joints for the reporting of human joint motion—part I: ankle, hip, and spine. International Society of Biomechanics. *J Biomech*. 2002;35:543-548.